PHYSICAL REVIEW B **81**, 245114 (2010)

NaAlSi: Self-doped semimetallic superconductor with free electrons and covalent holes

H. B. Rhee, S. Banerjee, E. R. Ylvisaker, and W. E. Pickett
Department of Physics, University of California, Davis, California 95616, USA
(Received 10 January 2010; revised manuscript received 21 May 2010; published 15 June 2010)

The layered ternary *sp* conductor NaAlSi, possessing the iron-pnictide "111" crystal structure, superconducts at 7 K. Using density-functional methods, we show that this compound is an intrinsic (self-doped) low-carrier-density semimetal with a number of unusual features. Covalent Al-Si valence bands provide the holes, and free-electronlike Al 3*s* bands, which propagate in the channel between the neighboring Si layers, dip just below the Fermi level to create the electron carriers. The Fermi level (and therefore the superconducting carriers) lies in a narrow and sharp peak within a pseudogap in the density of states. The small peak arises from valence bands which are nearly of pure Si, quasi-two-dimensional, flat, and coupled to Al conduction bands. Isostructural NaAlGe, which is not superconducting above 1.6 K, has almost exactly the same band structure except for one missing piece of small Fermi surface. Certain deformation potentials induced by Si and Na displacements along the *c* axis are calculated and discussed. It seems likely that the mechanism of pairing is related to that of several other lightly doped two-dimensional nonmagnetic semiconductors (TiNCl, ZrNCl, HfNCl), which is not well understood but apparently not of phonon origin.

DOI: 10.1103/PhysRevB.81.245114 PACS number(s): 71.20.−b, 74.20.Pq, 74.70.Ad

I. INTRODUCTION

The discovery of new superconductors in unexpected materials brings the potential to understand something deeper, or perhaps something different, about the underlying properties that favor superconducting pairing. The discovery of high-temperature superconductivity (to 56 K so far) in Fe pnictides[1] is a recent spectacular example, and is also an example of close relationships between magnetism and superconductivity, though the connections are still far from clear.

New superconductors where little or no magnetic effects are present are also arising, and these clearly involve different physics from the cuprate or Fe-pnictide high-temperature superconductors. Electron-doped *M*NCl, where *M*=Zr or Hf, becomes superconducting immediately upon undergoing the insulator-to-metal transition,[2–5] which, in the case of *M*=Hf, is higher than 25 K. The similarly layered, electron-doped, ionic insulator TiNCl superconducts up to 16 K. Magnetic behavior in these materials is at most subtle, amounting to an enhancement in Pauli susceptibility near the metal-to-insulator transition.[6]

In this paper we address the ternary silicide NaAlSi (space group $P4/nmm$, $Z=2$), another ionic and layered material that shows unexpected superconductivity, and does so in its native (without doping or pressure) stoichiometric state, at 7 K.[7] NaAlSi introduces new interest from several viewpoints. First, it is an *sp* electron superconductor, with a high T_c for such materials at ambient pressure. Pb is an *sp* superconductor with comparable T_c (7.2 K) but with simple metallic bonding and heavy atoms, making it very different. Doped Si (Ref. 8) and doped diamond[9] superconduct in the same range, and are of course very different classes of materials. A more relevant example is the pseudoternary compound $Ba_{1-x}K_xBiO_3$ (BKBO), which undergoes an insulator-to-metal transition for $x\approx 0.4$, beyond which its T_c surpasses 30 K.[10,11]

Second, the Al-Si layered substructure is like that of the Fe-As layer in the Fe-pnictide superconductors, raising the possibility of some connections between their electronic structures. In fact, NaAlSi has the same structure as the Fe-pnictide "111" compounds, with Al being tetrahedrally coordinated by Si (analogous to Fe being tetrahedrally coordinated by As). In spite of their structural similarities, these compounds have major differences; for example, the Fe pnictides are 3*d* electron systems with magnetism while NaAlSi is an *sp* electron system without magnetism.

Third, NaAlSi is the isovalent sister (one row down in the periodic table for each atom) of LiBC. LiBC itself is (in a sense) isovalent and also isostructural to MgB_2; however, due to the B-C alternation around the hexagon in the honeycomb-structure layer, LiBC is insulating rather than conducting. When hole doped while retaining the same structure, $Li_{1-x}BC$ has stronger electron-phonon coupling than does MgB_2.[12] While NaAlSi has a substantially different structure than LiBC, its isovalence and its combination of covalence with some ionic character is shared with LiBC.

Yet another closely related compound is CaAlSi, whose two different stacking polymorphs and parent structure superconduct in the 5–8 K range.[13,14] Linear-response and frozen-mode calculations indicate electron-phonon coupling is the likely mechanism; in particular, an ultrasoft phonon mode appears and is suggested to play a role in the superconductivity.[15–20] It is curious that in this compound, where divalent Ca (comparing it with NaAlSi) contributes one additional electron into the Al-Si *sp* bands, the preferred structure is that of AlB_2 (i.e., MgB_2) with sp^2 planar bonding[15,16,18] rather than the more sp^3-like bonding in NaAlSi. Electronic structure calculations show that CaAlSi has one electron in the conduction band above a bonding-antibonding band separation at the NaAlSi band-filling level, a situation which would not appear to be particularly favorable for sp^2 bonding.

In this paper we analyze first-principles electronic structure calculations that reveal that NaAlSi is a naturally self-doped semimetal, with doping occurring—thus charge transfer occurring—between covalent bands within the Al-Si

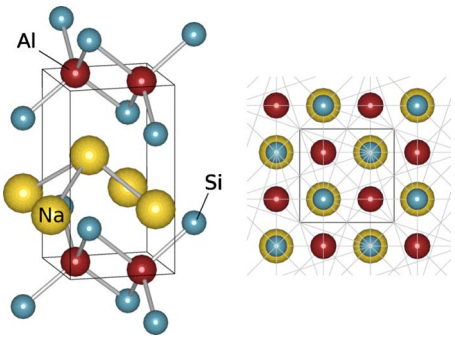

FIG. 1. (Color online) Crystal structure (Ref. 24) of NaAlSi. Four Si atoms tetrahedrally surround an Al atom, and these Al-Si networks sandwich the Na atoms. The unit cell is outlined in black.

substructure and two-dimensional (2D) free-electronlike bands within the Al layer. The resulting small Fermi surfaces (FSs) are unusual, complicated by the small but seemingly important interlayer coupling along the crystalline c axis.

II. COMPUTATIONAL METHODS

First-principles, local-density approximation calculations were carried out using the full-potential local-orbital scheme.[21] A k-point mesh of $20\times20\times12$ was used, and the Perdew-Wang 92 approximation[22] was applied for the exchange-correlation potential. The experimental lattice constants obtained by Kuroiwa *et al.*[7] (a=4.119 Å and c =7.632 Å) and internal coordinates published by Westerhaus and Schuster[23] (z_{Na}=0.622, z_{Si}=0.223) were used in our calculations.

III. ELECTRONIC STRUCTURE

A. Discussion of the band structure

The calculated band structure of NaAlSi is shown in Fig. 2. As expected, the Na ion gives up its electron to the Si-Al-Si trilayer (see Fig. 1), which may have some ionic character, though it is not easy to quantify (the valence bands have much more Si character than Al character, seemingly more than suggested by their number of valence electrons). There are several readily identifiable classes of bands. Two primarily Si 3s bands, with a small amount of Al 3s character, are centered 9 eV below the Fermi level ε_F and have a width of 2.5 eV. Above them there is a six-band complex of Al-Si s-p bands (heavily Si) that are very nearly filled, the band maximum only slightly overlapping ε_F.

Above ε_F lie nonbonding and antibonding bands, and the Na s bands. Among these there are a pair of distinctive bands, which can be identified most easily by their Al s character in the top panel of Fig. 2. These bands are nearly free-electronlike with large dispersions, and cross many other bands with little mixing. Along Γ-M they are degenerate and easily identifiable in Fig. 2, as they disperse up through the Fermi level to nearly 10 eV at the M point. Along Γ-X, and similarly at the top of the zone Z-R, they are distinct: one again disperses upward rapidly, cutting through many other bands, also to nearly 10 eV at X; the other disperses much more weakly to X, with a bandwidth of about 2 eV. Their Al s character and nearly vanishing Si character identify these as free-electron states, in which electrons move down channels of Al atoms separately in x and y directions. (Note that their lack of k_z dispersion identifies them as planar bands.) There is some coupling to the states in a parallel channel of Al atoms, giving rise to the 2 eV transverse dispersion. These bands lie 0.5 eV below ε_F at Γ and contain electrons. Without interference with other bands near the Fermi level and supposing them to be isotropic in the plane (but see below), such FSs might include 3%–4% of the area of the zone, which would equate to an intrinsic electron doping for two bands, both spins of around 0.12–0.16 carriers per unit cell, and the concentration of hole carriers would be equal. The anisotropy, discussed below, makes the actual carrier concentration much lower.

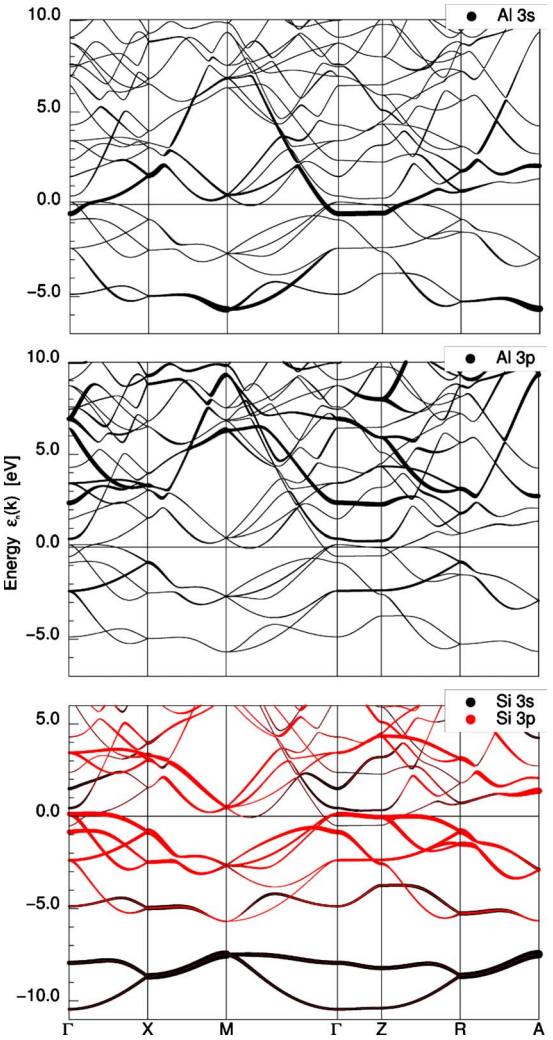

FIG. 2. (Color online) Band structure, with projected fatbands, of NaAlSi. Top panel: the Al 3s character of bands is indicated by broadening. A doubly degenerate pair of broad bands is evident along the Γ-M direction. Middle panel: Al 3p character is weak below 2–3 eV. Bottom panel: Si 3s (black) bands below −8 eV, and Si 3p in the valence bands and lower conduction bands.

The small overlap of valence and conduction bands results in semimetallic character and small Fermi surfaces. The

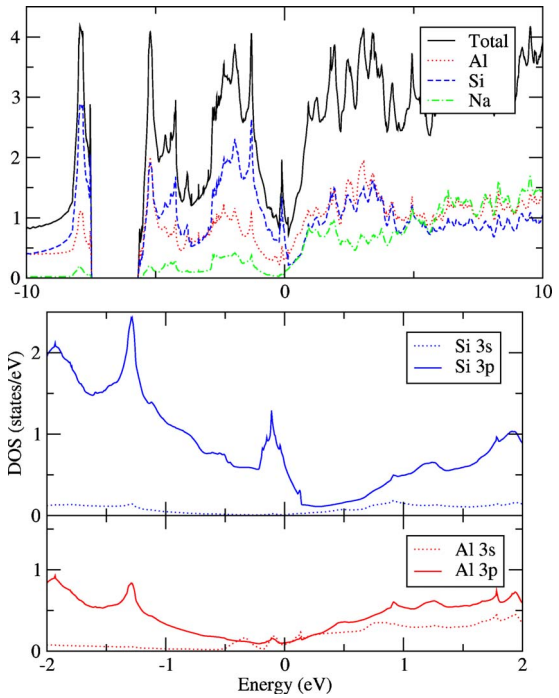

FIG. 3. (Color online) Total and partial (atom- and orbital-projected) DOSs of NaAlSi. Top panel: total (states per electron volt per unit cell) and atom-projected DOS in a 20 eV wide region, showing the pseudogap centered at the Fermi level (the zero of energy) punctuated by the curiously narrow and sharp peak at the Fermi level. Middle panel: expanded view of the peak, and the variation in the DOS near the Fermi level, separated into Si s and p contributions. Lower panel: the Al s and p character; the onset of s character occurs just below the Fermi level.

valence bands are quite anisotropic. Looking at the valence bands along Γ-X, one might try to characterize them as one "heavy-hole" and one "light-hole" band, degenerate at Γ, with the band maximum lying 0.13 eV above ε_F. However, the heavy-hole band is actually almost perfectly flat for the first third of the Γ-X line, before dispersing downward across ε_F and farther below. Due to this flatness, the band cannot be characterized by an effective mass. The conduction bands contribute the pair of light electron bands described above. In addition, one conduction band dips slightly below the Fermi level along Γ-M near M.

The fatbands representation in Fig. 2 that reveals the dominant band character shows that the Si $3p_x$ and $3p_y$ orbitals dominate the valence states near ε_F. As anticipated from consideration of the layered structure as mentioned earlier, the electronic structure is quasi-2D, with generally small dispersion along k_z near ε_F. However, the small k_z dispersion of one band is important in determining the geometry of the FSs, as discussed in more detail below.

B. Density of states

Figure 3 shows the total, partial, and projected densities of states (DOS) of NaAlSi, in units of states per electron volt per unit cell. The Na contribution near the Fermi level is negligible and thus not shown. Except for a strong dip

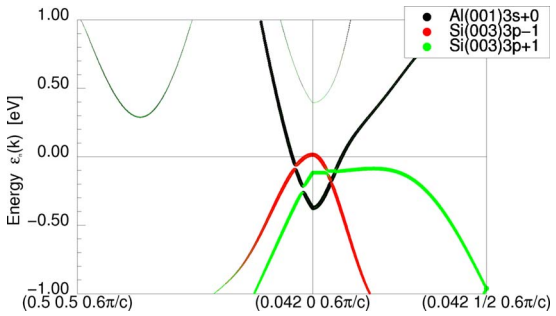

FIG. 4. (Color online) Bands along two lines in the $k_z=0.6\pi/c$ plane, near the Fermi level, showing a flat band (one of the two Si-derived valence bands) lying at the energy of the DOS peak.

("pseudogap") near the Fermi level and a less severe dip in the −3 to −4 eV range, the DOS hovers around 3 states/eV throughout both valence and conduction bands. Within the pseudogap encompassing the Fermi energy, there is an anomalous sharp and narrow peak with ε_F lying on its upper slope, as noted previously by Kuroiwa *et al.*[7] The value of $N(\varepsilon_F)$ is 1.1 states/eV (both spins). We discuss below the FSs of both hole (Si) and electron (Al) character.

It seems clear that the transport properties and low-energy properties (which have not yet been reported), and in particular the superconductivity of NaAlSi, are intimately associated with this sharp and narrow peak in the DOS, which includes the Fermi level. The projected DOS shows the flat bands (see also Fig. 4) that give rise to this peak are strongly Si derived. There is Al $3s$ character that turns on just below ε_F but it is relatively small compared to the Si character at ε_F, and its magnitude remains low and nearly constant through the peak. There is Al $3p$ character of the same magnitude in the vicinity of the Fermi level.

Due to the curious nature of the peak and its importance because it lies very near ε_F, we have investigated its origin. The top edge of the peak coincides with the flat band along Γ-X at 0.13 eV. The width of the peak, about 0.35 eV, must be due to dispersion and band mixing away from the symmetry lines. Since these effects are not evident in the band structure, we have examined the bands off symmetry lines, and specifically in the $k_z=0.6\pi/c$ plane, since this is the value of k_z where the weakly dispersing band near ε_F crosses the Fermi level. The bands in two directions in the plane, from $(0.042\pi/a, 0, 0.6\pi/c)$ to two zone-boundary points are pictured in Fig. 4. The Al-derived conduction band is highly dispersive, and moreover hardly mixes with the valence bands, so it is not relevant. Although only $0.042\pi/a$ off the Γ-Z line, the valence bands' degeneracy is split by 0.2 eV, and in the k_x direction one band is strongly dispersive downward while the other is flat halfway across the zone, as is also the case for $k_z=0$ (the original band-structure plot). It is this region of the zone, and this band, that contributes to the peak, and is not due to mixing of bands but rather to small but important disperion along k_z but practically no dispersion in k_x until halfway across the zone.

Nonetheless, the slope of the DOS at ε_F is rather steep, and this feature, along with the low value of $N(\varepsilon_F)$, may give rise to high thermopower for the material, as often occurs in doped semiconductors. The standard low-temperature limit

of thermopower (the Seebeck coefficient tensor) $\mathbf{S}(T)$ in semiclassical Bloch-Boltzmann theory is

$$\mathbf{S}(T) \to -\frac{\pi^2 k_B}{3e} \frac{d \ln \boldsymbol{\sigma}(\varepsilon)}{d\varepsilon}\bigg|_{\varepsilon_F} k_B T. \tag{1}$$

The conductivity tensor $\boldsymbol{\sigma}(\varepsilon)$ can be written in terms of the average velocity $[\vec{v}(\varepsilon)]$ product, DOS, and scattering time $\tau(\varepsilon)$ over the constant energy (ε) surface

$$\boldsymbol{\sigma}(\varepsilon) = 4\pi e^2 \langle \vec{v}(\varepsilon)\vec{v}(\varepsilon)\rangle N(\varepsilon)\tau(\varepsilon). \tag{2}$$

The thermopower thus picks up contributions from the energy variation in three quantities: the dyadic product $\langle \vec{v}\vec{v}\rangle$, $N(\varepsilon)$, and $\tau(\varepsilon)$. Often the energy dependence of τ is neglected, out of lack of detailed knowledge, though it also can be argued to follow roughly $1/\tau(\varepsilon) \propto N(\varepsilon)$ for elastic scattering. The energy dependence of $v^2(\varepsilon)$ also counteracts the energy dependence of $N(\varepsilon)$. Nevertheless it is observed that materials with large slope in $N(\varepsilon)$ frequently have large thermopower. For NaAlSi we calculate $d \ln N(\varepsilon)/d\varepsilon|_{\varepsilon_F} = -4.0\ \mathrm{eV}^{-1}$. This value can be compared with other materials that have fine structure near the Fermi level: $TiBe_2$, where $d \ln N(\varepsilon)/d\varepsilon|_{\varepsilon_F} = 10-12\ \mathrm{eV}^{-1}$ and $N(\varepsilon_F)$ also is much larger;[25] and $MgCNi_3$ with its very impressive peak very near ε_F, for which $d \ln N(\varepsilon)/d\varepsilon|_{\varepsilon_F}$ ranges from -15 to $-20\ \mathrm{eV}^{-1}$.[26]

For a diagonal conductivity tensor, as is the case here, the energy derivative of diagonal elements of $\boldsymbol{\sigma}$ that occurs in Eq. (1) can also be expressed, straightforwardly from the expression given by Ashcroft and Mermin[27] following an integration by parts, as

$$\frac{1}{\sigma}\frac{d\sigma}{d\varepsilon} = \frac{d \ln \tau(\varepsilon)}{d\varepsilon} + \mathcal{M}^{-1}(\varepsilon)[v^2(\varepsilon)]^{-1}, \tag{3}$$

where $\mathcal{M}^{-1}(\varepsilon)$ is (a diagonal element of) the inverse mass tensor (second derivative of ε_k) averaged over the constant energy surface. This expression provides an alternate viewpoint to the usual expression follow from the equations above,

$$\frac{d \ln \sigma}{d\varepsilon} = \frac{d \ln \tau(\varepsilon)}{d\varepsilon} + \frac{d \ln v^2}{d\varepsilon} + \frac{d \ln N(\varepsilon)}{d\varepsilon} \tag{4}$$

and this latter expression is more stable to evaluate numerically.

For any quantitative estimate for a semimetal, the expression must be generalized to two-band form (electrons and holes). The valence and conduction bands have differing signs of their effective masses, and for NaAlSi the effective mass $\mathcal{M}$ will be energy dependent (the bands are not simply parabolic at $E(\varepsilon_F)$). The energy variation in the scattering time for elastic scattering might lead to a simplification since it should be dominated by the availability of final states, i.e.,

$$\frac{d \ln \tau(\varepsilon)}{d\varepsilon} \approx \frac{d \ln N(\varepsilon)}{d\varepsilon} \tag{5}$$

holding separately for electrons and holes.

A significant complication arises, however, because the thermopower is not a response function itself but rather the ratio of two response functions, each of which involves a sum over bands. In addition, the temperature dependence of the electron and hole chemical potentials (hence carrier densities) are coupled. Even in the simple case of a semimetal arising from quadratic bands, the expressions lose any pedagogic value, although their evaluations require modest numerical calculations.[28] The generalization to nonquadratic bands as in NaAlSi is beyond the scope of this paper, though a measurement of the thermopower might make it worthwhile to perform the calculation and make the comparison.

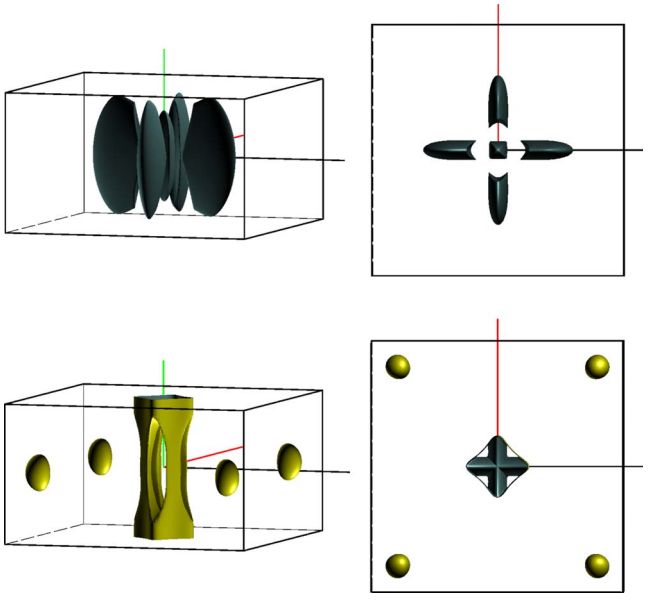

FIG. 5. (Color online) Views from the *xy* plane (left) and top (right) of the FSs of NaAlSi, centered at Γ. The blue (dark) surfaces enclose holes and the yellow (light) surfaces enclose electrons.

C. Unusual Fermi surfaces

Figure 5 depicts the calculated FSs. In spite of the generally 2D band structure, the small k_z dispersion of bands at ε_F make some of the FSs surprisingly three dimensional. Electron pockets and hole pockets coexist in the Brillouin zone, with electron and hole concentrations necessarily being equal.

Hole surfaces. Four hole "fan-blade" surfaces lie oriented in the *xz* and *yz* planes. At the center, extending from Γ halfway to Z, lies a long and narrow surface with square cross section. The top view allows the origin of these surfaces to be understood. The cross sections in the *xy* plane are of two ellipses that are very anisotropic (in the *xy* plane) and at right angels to each other. Each corresponds to a dispersion that is weak in one direction (the long major axis) and strong in the other (minor axis). These bands would intersect but in fact are intersected by the electron band that cuts a squarish hole (rotated by 45°), within which the elongated hole surface inside re-emerges.

Electron surfaces. In the bottom panels of Fig. 5, the squarish electron surface (with k_z variation and resulting holes, shown in the lower two panels of Fig. 5) that cuts the aforementioned hole surface is pictured, and substantiates

the discussion provided just above. In addition, there are simple electron ellipsoids centered along the Γ-M lines. It is curious that in a band structure that is for the most part strongly 2D, all the FSs have a rather definite three-dimensional character. Although the bands show little dispersion along Γ-Z, the bands just above the Fermi level are quite different depending on whether $k_z=0$ or $k_z=\pi$. In particular, the lowest band along R-A is rather flat but the lowest conduction band along X-M has a dispersion of nearly 2 eV. Similar comparisons can be made for the bands along Γ-X and Z-R. The k_z dispersion is not nearly as strong near $k_x=k_y=0$, which is clear from both the band structure and the FS.

Short discussion. It was noted in the Sec. I that the NaAlSi structure is the same as the Fe-pnictide "111" structure. Moreover, in both compounds, the relevant bands involve only the (Si-Al-Si or As-Fe-As) trilayer. The top view of the fan-blade surfaces have characteristics in common with those of some of the Fe pnictides,[29,30] all of which have this same trilayer. The similarity is that the top view of the fan blades (if one ignores the diamond-shaped cutout at the intersection, centered at Γ) appears to show intersecting FSs, neither of which has the square symmetry of the lattice.

Such occurrence of intersecting FSs, each with lower symmetry than the lattice, has been analyzed for LaFeAsO (a "1111" compound) by Yaresko *et al.*[31] A symmetry of the Fe_2As_2 (also Al_2Si_2) substructure is a nonprimitive translation connecting Fe atoms (respectively, Al atoms) followed by z reflection. This operation leads to symmetries that allow $k_z=0$ bands to be unfolded into a larger Brillouin zone (that is, a "smaller unit cell" having only one Fe atom) which unfolds the band structure and the intersecting FSs. The NaAlSi FSs appear to have this similar crossing (albeit interrupted by the free-electron bands), and the highly anisotropic dispersion is due to distinct (but symmetry related) hopping along each of the crystal axes. In this respect NaAlSi may clarify the electronic structure of the pnictides: by analogy, there are separate bands that disperse more strongly along the (1,1) direction or the (1,−1) direction, and give rise to the intersecting, symmetry-related surfaces. In NaAlSi the bands are much more anisotropic in the plane (approaching one dimensional), making such character much clearer. A difference that complicates the analogy is that in the pnictides the bands near ε_F are derived from the Fe atoms, which comprise the center layer of the trilayer, whereas in NaAlSi the bands under discussion are derived from the Si atoms, which comprise the two outer layers.

D. Wannier functions

Pictured in Fig. 6 are symmetry-projected Wannier functions (WFs) projected onto Si $3p$ orbitals. The extension of the WFs shows considerable involvement from nearby Al and Si atoms, and in addition have some density extending into the Na layers. The p_x WF consists of an atomic p_x function, with its density shifted downward by the bonding contribution of Al sp^3 hybrid orbitals. Beyond the p_x lobes the nearest Si atoms form a bonding lobe that connects to the "small" side of the Al sp^3 function. The large p_x lobes and

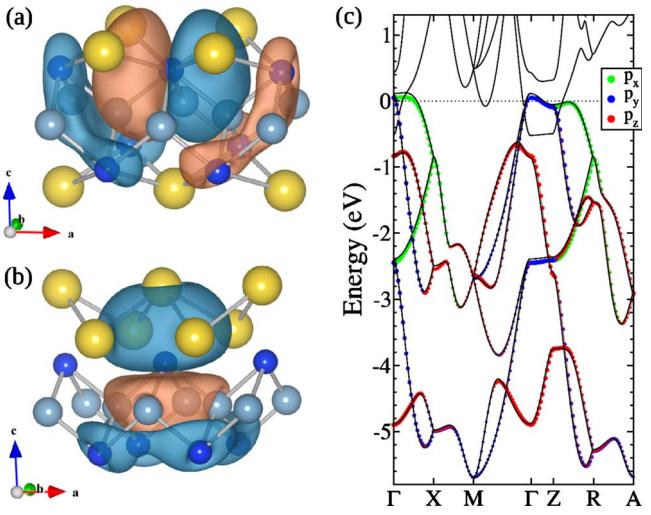

FIG. 6. (Color online) Isosurface of the WFs for (a) Si $3p_x$ and (b) Si $3p_z$. Na atoms are large and yellow (light) colored, Si atoms are small and blue (dark) colored. The two colors of the isosurface represent different signs. (c) The tight-binding fatbands band structure described in the text for the WFs, compared to the DFT band structure (black lines).

the extra contribution from nearby Si atoms are responsible for the largest hopping amplitudes shown in Table I, although there is some phase cancellation between the p_x lobe and the lobe lying beyond the nodal surface.

The p_z WF has one lobe extended well into the Na layer; this is responsible for the largest hoppings along $\mathbf{b}^*$ in Table I, and they create the large dispersion in the p_z bands seen in Fig. 6(c). Again, the Al atoms contribute with an sp hybrid orbital, although it appears to be more sp^2-like than sp^3-like. There is also a "ring" structure below the Al layer, where an sp hybrid orbital from the Si atoms forms a bonding combination but it is antibonding with the p_z function on the central Si. The largest contribution to near-neighbor hopping in the Al-Si plane between p_z and p_x or p_z is most likely due to this ring structure, as the p lobes are confined to the inside of

TABLE I. Selected hopping integrals in millielectron volt for the Si $3p$ WFs along the vectors $\mathbf{a}=(a,0,0)$ (hopping within a Si layer), $\mathbf{b}=(a/2,a/2,d)$ (hopping across an Al layer), and $\mathbf{b}^*=(a/2,a/2,c-d)$ (hopping across a Na layer). d is the distance in the z direction between Si atoms above and below Al planes.

		p_x	p_y	p_z
a	p_x	761		60
	p_y		−62	60
	p_z	60	60	−40
2**a**	p_x	128		27
b	p_x	361	300	360
	p_y	300	361	360
	p_z	360	360	360
$\mathbf{b}^*$	p_x	12	5	50
	p_y	5	12	50
	p_z	50	50	185

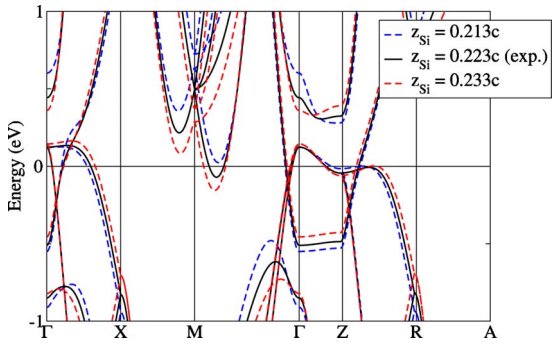

FIG. 7. (Color online) Comparison of band structures near ε_F for different z_{Si} values.

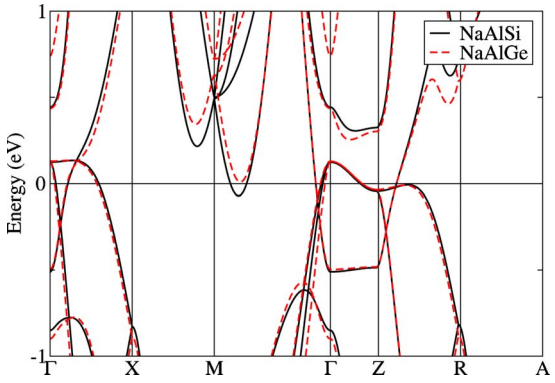

FIG. 8. (Color online) Blowup of the band structures of NaAlSi and NaAlGe near ε_F.

a square of near-neighbor Al atoms, which are only edge sharing with the nearest Si atoms along **b** vectors. This is the likely reason that all the hoppings along **b** are approximately of the same magnitude. The dispersion which creates the FSs along Γ-Z (seen in Fig. 5) is composed only of the p_x and p_y WFs. This is not caused by the large hoppings but by smaller hoppings along $\mathbf{b}^*$ between p_x and p_y WFs. Without these small hoppings, the band just above ε_F is dispersionless along Γ-Z.

IV. RESPONSE TO CHANGES

A. Electron-ion coupling

A deformation potential $\mathcal{D}$ is the shift in an energy band with respect to sublattice atomic displacement. One can freeze in phonon modes to calculate deformation potentials, which at the FS are directly connected to electron-phonon matrix elements.[32]

Moving the Si atoms in the z direction by $\pm 1\%$ of the experimental parameter, such that the tetrahedra surrounding the Al atoms stretch or flatten (while remaining centered on Al), gives an average deformation potential of ~ 0.8 eV/Å over five band positions near the Fermi level. The largest shift is for the ellipsoidal electron pockets, with $\mathcal{D} \sim 1.2$ eV/Å. These ellipsoids disappear when the Si atoms are displaced toward the Al plane (see Fig. 7).

Flattening the Na bilayer, so as to remove the buckling of the Na atoms, requires a (very large) 12% change in the z component of the Na atoms. We chose such a large displacement because we do not expect a substantial deformation potential for Na movement. Even this large displacement does not alter very much the valence bands, as expected, and the hole FSs remain virtually unchanged. The conduction bands at the Fermi level, however, shift appreciably, resulting in a modulation of the electron ellipsoids along (1,1) near M. In addition, the accidental four band near degeneracy that is 0.5 eV above ε_F at M splits the two separate doubly degenerate states, opening up a gap of ~ 0.7 eV, which is equivalent to a deformation potential of ~ 0.8 eV/Å (but the bands are not at ε_F).

These values of $\mathcal{D}$ are very small when compared to that of the E_{2g} phonon mode in MgB_2, which has a value of 13 eV/Å.[33] The C atom displacements in B-doped diamond (T_c=4 K) give rise to two large deformation potentials of 14 and 7 eV/Å.[34] However, these are the largest values known, far larger than in several good superconductors. In Li_2Pt_3B, a superconductor at T_c=8 K, the deformation potential was calculated for Pd motions in the ⟨011⟩ direction. For about 25 calculated values near the Fermi surface, the mean value was $\mathcal{D}$=1.15 eV/Å, with values covering a wide range from 0.15 to 4 eV/Å.[35] Values for motions of the Li atom in this compound were about an order of magnitude smaller. The values we calculate for NaAlSi are comparable to the mean value for Pt motion in Li_2Pt_3B, which is not certain to be phonon coupled but for which no serious alternative has been suggested. The large variation calculated in Li_2Pt_3B warns against drawing any conclusions from a small sample.

B. Magnetic susceptibility

The magnetic spin susceptibility χ is given by

$$\chi = \frac{\partial M}{\partial H} = (\partial^2 E/\partial M^2)^{-1}.$$

Fixed-spin-moment calculations were conducted to produce an energy vs moment $E(M)$ curve, resulting in a susceptibility of $\chi = 1.30\mu_B^2$ eV^{-1} per unit cell (uc). Using the calculated bare Pauli susceptibility $\chi_0 = 1.11\mu_B^2$ eV^{-1}, exchange enhancement of the susceptibility is

$$S = \frac{\chi}{\chi_0} = 1.17.$$

A small enhancement of roughly this magnitude (17%) is expected for an *sp* metal; for comparison, Janak[36] obtained the value S=1.34 for Al directly from density-functional theory in the $H \to 0$ limit.

C. Comparison to NaAlGe

Isostructural and isovalent NaAlGe is not superconducting (above 1.6 K, at least), so it should be instructive to compare its electronic structure to that of NaAlSi. Using the experimental lattice and internal parameters of NaAlGe,[23] we have calculated its band structure and compared it with that of NaAlSi on a rather fine scale in Fig. 8. The band structures are extremely similar near ε_F, the only noticeable difference

being that the band along Γ-M near M does not cross ε_F in NaAlGe. The free-electron band is also identical.

Supposing (first) the tiny bit of FS along Γ-M cannot account for the difference in superconducting behaviors, the factors relevant for electron-phonon coupling will be the difference in mass (Ge is more than twice as heavy as Si) and the difference in electronic character, which can affect force constants and electron-phonon matrix elements. Thus electron-phonon coupling that is concentrated in the Si vibrations might be consistent with the decrease (or disappearance) in T_c. However, an electron-phonon coupled semimetal with $T_c=7$ K would be remarkable.

Another possibility, especially considering the low-energy electronic behavior to be expected in a two-dimensional compensated semimetal with low-carrier density, is that the pairing mechanism is electronic rather than phononic. In three dimensions purely electronic pairing mechanisms have attracted serious study (albeit in the homogeneous electron-gas approximation, by Sham and collaborators,[37,38] for example). However, 2D semimetals introduce new features that deserve detailed study, such as the 2D plasmon that goes to zero as $\sqrt{q}$. A model in which the electronic response of a 2D electronic superlattice plays a central role in the mechanism has been previously studied[39,40] using a model of parallel conducting sheets separated by a dielectric spacer. This model may be useful as a starting point for understanding NaAlSi, with or without phonon processes.

Another possibility is that the small FS pockets are important. In the scenario that superconductivity arises from an enhancement of electron-phonon coupling, it would require a new and unusual contribution of a small density of additional electrons with nonadiabatic coupling to phonons. These tiny pockets will contribute additional low-frequency electronic response as well, including low-frequency plasma oscillations, intervalley electron-hole polarization at large momentum, and additional interband transitions. As noted in the Sec. I, NaAlSi adds another low-carrier density, two-dimensional system to the list of unusual and unexplained superconductors, and it may be especially useful for further study specifically for the reason that it does not contain any transition metal.

V. CONCLUDING REMARKS

The classes of materials that contain relatively high-temperature superconductors[41] continues to expand. Superconductors derived from doped 2D semiconductors pose many of the most interesting issues in superconductivity today. The cuprates and the Fe pnictides (and chalcogenides) are strongly magnetic, and comprise one end of the spectrum (though they are themselves quite different). On the other end lie those with little, perhaps negligible, magnetism: electron-doped ZrNCl and HfNCl, and electron-doped TiNCl. There are several other, lower-T_c systems, whose behavior seems different still (hydrated Na_xCoO_2, $Li_{1-x}NbO_2$, and several transition-metal disulfides and diselenides).

A common feature of most of these systems is that they have strong 2D features and have a small but not tiny (as in superconducting doped $SrTiO_3$) concentration of charge carriers, often in the range of 0.05–0.15 carriers per uc. These materials also have ionic character, although in the Fe pnictides and NaAlSi the ionic character is not easily quantified. NaAlSi differs from the other mentioned superconductors in that it has *sp* carriers—the others have carriers in *d* bands—and it is self-doped, being a compensated semimetal. Our results suggest that a useful view of NaAlSi is that it be regarded as arising from an underlying ionic semiconductor but that it has a small *negative* gap rather than a true gap. Without the overlap of the valence and conduction bands, it would be a 2D, partially ionic, partially covalent semiconductor such as the aforementioned nitridochloride compounds, which superconduct in the 15–25 K range. Comparing the characteristics of these two classes of superconductors should further the understanding of 2D superconductivity.

A further distinction of NaAlSi is that, in spite of a strongly 2D band structure overall, the small k_z dispersion of the doubly degenerate band at the Fermi level gives three-dimensional Fermi surfaces. One of these two bands also has extremely strong anisotropy within the 2D plane, especially for a compound with tetragonal symmetry, which further serves to produce intricate Fermi surfaces and contributes to the peculiar peak in the density of states at ε_F.

In summary, NaAlSi contains a number of peculiarities compared to related superconductors with strongly layered structure, and it seems certain that the pairing mechanism, whether phononic or electronic, will require an increase in understanding of the relatively low-energy electronic behavior in this compensated semimetal. Further study of this compound should help to generalize our understanding of superconductivity in low-density, layered materials.

ACKNOWLEDGMENTS

This work was supported by DOE Grant No. DE-FG02-04ER46111, the Strategic Sciences Academic Alliance Program under Grant No. DE-FG03-03NA00071, and by DOE SciDAC Grant No. DE-FC02-06ER25794.

[1] Y. Kamihara, T. Watanabe, M. Hirano, and H. Hosono, J. Am. Chem. Soc. **130**, 3296 (2008).
[2] S. Yamanaka, H. Kawaji, K. Hotehama, and M. Ohashi, Adv. Mater. **8**, 771 (1996).
[3] S. Shamoto, T. Kato, Y. Ono, Y. Miyazaki, K. Ohoyama, M. Ohashi, Y. Yamaguchi, and T. Kajitani, Physica C **306**, 7 (1998).
[4] S. Yamanaka, K. Hotehama, and H. Kawaji, Nature (London) **392**, 580 (1998).
[5] S. Shamoto, K. Iizawa, M. Yamada, K. Ohoyama, Y. Yamaguchi, and T. Kajitani, J. Phys. Chem. Solids **60**, 1431 (1999).

[6] S. Yamanaka, T. Yasunaga, K. Yamaguchi, and M. Tagawa, J. Mater. Chem. **19**, 2573 (2009).
[7] S. Kuroiwa, H. Kawashima, H. Kinoshita, H. Okabe, and J. Akimitsu, Physica C **466**, 11 (2007).
[8] E. Bustarret, C. Marcenat, P. Achatz, J. Kačmarčik, F. Lévy, A. Huxley, L. Ortéga, E. Bourgeois, X. Blase, D. Débarre, and J. Boulmer, Nature (London) **444**, 465 (2006).
[9] E. A. Ekimov, V. A. Sidorov, E. D. Bauer, N. N. Mel'nik, N. J. Curro, J. D. Thompson, and S. M. Stishov, Nature (London) **428**, 542 (2004).
[10] L. F. Mattheiss, E. M. Gyorgy, and D. W. Johnson, Jr., Phys. Rev. B **37**, 3745 (1988).
[11] S. Jin, T. H. Tiefel, R. C. Sherwood, A. P. Ramirez, E. M. Gyorgy, G. W. Kammlott, and R. A. Fastnacht, Appl. Phys. Lett. **53**, 1116 (1988).
[12] H. Rosner, A. Kitaigorodsky, and W. E. Pickett, Phys. Rev. Lett. **88**, 127001 (2002).
[13] H. Sagayama, Y. Wakabayashi, H. Sawa, T. Kamiyama, A. Hoshikawa, S. Harjo, K. Uozato, A. K. Ghosh, M. Tokunaga, and T. Tamegai, J. Phys. Soc. Jpn. **75**, 043713 (2006).
[14] S. Kuroiwa, H. Sagayama, T. Kakiuchi, H. Sawa, Y. Noda, and J. Akimitsu, Phys. Rev. B **74**, 014517 (2006).
[15] I. R. Shein, N. I. Medvedeva, and A. L. Ivanovskii, J. Phys.: Condens. Matter **15**, L541 (2003).
[16] G. Q. Huang, L. F. Chen, M. Liu, and D. Y. Xing, Phys. Rev. B **69**, 064509 (2004).
[17] I. I. Mazin and D. A. Papaconstantopoulos, Phys. Rev. B **69**, 180512(R) (2004).
[18] M. Giantomassi, L. Boeri, and G. B. Bachelet, Phys. Rev. B **72**, 224512 (2005).
[19] R. Heid, K.-P. Bohnen, B. Renker, P. Adelmann, T. Wolf, D. Ernst, and H. Schober, J. Low Temp. Phys. **147**, 375 (2007).
[20] S. Kuroiwa, A. Q. R. Baron, T. Muranaka, R. Heid, K. -P. Bohnen, and J. Akimitsu, Phys. Rev. B **77**, 140503(R) (2008).
[21] K. Koepernik and H. Eschrig, Phys. Rev. B **59**, 1743 (1999).
[22] J. P. Perdew and Y. Wang, Phys. Rev. B **45**, 13244 (1992).
[23] W. Westerhaus and H. U. Schuster, Z. Naturforsch. B **34**, 352 (1979).
[24] K. Momma and F. Izumi, J. Appl. Crystallogr. **41**, 653 (2008).
[25] A. B. Kyker and W. E. Pickett, Phys. Rev. B **71**, 224517 (2005).
[26] H. Rosner, R. Weht, M. D. Johannes, W. E. Pickett, and E. Tosatti, Phys. Rev. Lett. **88**, 027001 (2001).
[27] N. W. Ashcroft and N. D. Mermin, *Solid State Physics* (Harcourt Brace, New York, 1976), Eq. (13.65).
[28] K. Durczewski and M. Ausloos, Z. Phys. B **85**, 59 (1991).
[29] D. J. Singh, Phys. Rev. B **78**, 094511 (2008).
[30] I. I. Mazin, D. J. Singh, M. D. Johannes, and M. H. Du, Phys. Rev. Lett. **101**, 057003 (2008).
[31] A. N. Yaresko, G.-Q. Liu, V. N. Antonov, and O. K. Andersen, Phys. Rev. B **79**, 144421 (2009).
[32] F. S. Khan and P. B. Allen, Phys. Rev. B **29**, 3341 (1984).
[33] J. M. An and W. E. Pickett, Phys. Rev. Lett. **86**, 4366 (2001).
[34] K.-W. Lee and W. E. Pickett, Phys. Rev. Lett. **93**, 237003 (2004).
[35] K.-W. Lee and W. E. Pickett, Phys. Rev. B **72**, 174505 (2005).
[36] J. F. Janak, Phys. Rev. B **16**, 255 (1977).
[37] H. Rietschel and L. J. Sham, Phys. Rev. B **28**, 5100 (1983).
[38] M. Grabowski and L. J. Sham, Phys. Rev. B **29**, 6132 (1984).
[39] A. Bill, H. Morawitz, and V. Z. Kresin, Phys. Rev. B **66**, 100501(R) (2002).
[40] A. Bill, H. Morawitz, and V. Z. Kresin, Phys. Rev. B **68**, 144519 (2003).
[41] W. E. Pickett, Physica B **296**, 112 (2001).